J. Cell. Mol. Med. Vol 13, No 8B, 2009 pp. 1809-1822

Proteomics analysis of protein expression and specific protein oxidation in human papillomavirus transformed keratinocytes upon UVB irradiation

Marzia Perluigi [a, *], Alessandra Giorgi [a], Carla Blarzino [a], Federico De Marco [b], Cesira Foppoli [c], Fabio Di Domenico [a], D. Allan Butterfield [d], M. Eugenia Schininà [a], Chiara Cini [a], Raffaella Coccia [a]

[a] Department of Biochemical Sciences, "Sapienza" University of Rome, Rome, Italy
[b] Laboratory of Virology, "Regina Elena Institute for Cancer Research", Rome, Italy
[c] CNR Institute of Molecular Biology and Pathology, Rome, Italy
[d] Department of Chemistry, Center of Membrane Science, and Sanders-Brown Center on Aging, University of Kentucky, Lexington, KY, USA

Received: April 29, 2008; Accepted: August 1, 2008

Abstract

Increasing evidence supports the role of oxidative stress in cancer development. Ultraviolet (UV) irradiation is one of the major sources of oxidative stress through the generation of reactive oxygen species (ROS). Besides the physiological function of ROS in cellular homeostasis, accumulating reports suggest that ROS are involved in all stages of multistep cancer development. In order to investigate the involvement of oxidative damage into the mechanisms of tumour progression, we used a parallel proteomic approach to analyse the protein expression profile and to identify oxidatively modified proteins in human papillomavirus (HPV)-transformed keratinocytes (HK-168 cells) upon ultraviolet B (UVB) exposure. The HK-168 cells were obtained from normal human epidermal keratinocytes transfected with the whole genome of the high-risk HPV type 16, unanimously recognized as an etiological agent of cervical carcinoma. Because of its year-long latency, this tumour offers a convenient model to study the role of environmental concurring agents in the multistep malignant progression. By the protein expression profile, we identified 21 proteins that showed different expression levels in HK-168 cells treated with UVB in comparison with untreated cells. Focusing on the oxidative modifications occurring at the protein level, we identified five proteins that showed elevated protein carbonyls levels: α-enolase, heat shock protein 75, annexin 2, elongation factor Tu and elongation factor γ. Our results indicate that UVB-induced oxidative stress perturbs the normal redox balance and shifts HPV-transformed keratinocytes into a state in which the carbonylation of specific proteins is systematically induced. We suggest that UVB-induced modulation of protein expression combined with oxidative modification lead to protein dysfunction that might contribute to the malignant progression of transformed cells.

Keywords: proteomics • oxidative stress • HPV • cervical carcinoma

Introduction

The development of cancer in human beings and animals is a multistep process. The complex series of cellular and molecular changes participating in cancer development are mediated by a variety of endogenous and exogenous stimuli. A very powerful and ubiquitous cancer-promoting stimulus is that arising from reactive oxygen species (ROS) [1–3]. ROS are generated in normal physiologic processes, including aerobic metabolism, inflammation and immune response and are known to play a dual role in biological systems resulting either in beneficial or in harmful effects to living systems. Low concentrations or transient exposure to ROS induce cell proliferation and regulate the activation of several signalling pathways [4, 5]. In contrast, at high concentrations, ROS are important mediators of damage to cell structures, including lipids and membranes, proteins and nucleic acids [6]. The harmful effects of ROS are balanced by the antioxidant action of non-enzymatic

*Correspondence to: Marzia PERLUIGI, Ph.D.,
Department of Biochemical Sciences, "Sapienza"
University of Rome – P.le A. Moro, 5 – 00185 Rome, Italy.
Tel.: +39-06-49910900
Fax: +39-06-4440062
E-mail: permarzia@hotmail.com

doi:10.1111/j.1582-4934.2008.00465.x

antioxidants in addition to antioxidant enzymes. Despite the presence of the cell antioxidant defence system to counteract oxidative stress conditions, oxidative damage accumulates during the life cycle, and ROS-mediated damage to DNA, to proteins and to lipids has been proposed to play a key role in the development of many degenerative diseases including cancer [7].

The carcinogenic process can be described as an imbalance between cell proliferation and cell death shifted towards cell proliferation. Indeed mutations resulting in dysfunctional signalling pathways are hallmarks of cancerous cells and represent critical steps in the malignant progression. Increased ROS levels are well documented in transformed cells [8, 9] and have been implicated in the carcinogenic process through the regulation of a redox sensitive network controlling both cell proliferation and cell death pathways [10–13].

Cervical cancer, which continuously plagues many women all over the world, still remains to be one of the major focuses of researchers. Infection with human papilloma virus (HPV) has been implicated as an important aetiological factor in the causation of cervical cancer [14] and the role of HPV in association with other factors has been extensively studied [15, 16]. Large body of knowledge already generated in this area supports the view that high-risk HPV types, among which HPV-16 is the most prevalent type, have the ability to transform normal cells into a malignant phenotype. However, viral oncogenes expression, although necessary, is not *per se* sufficient to induce cancer as indicated by the frequent spontaneous clearance of HPV infection and the long delay between the onset of persistent infection and the emergence of the malignancy. Therefore other factors have to be involved in the progression of transformed cells to the full neoplastic phenotype. In the search of cancer promoting co-factors, several studies focused on the role of concurrent genital infections, racial and genetic characteristics and viral variants, but little attention has been paid to oxidative stress and its role in the process of neoplastic progression.

The aim of the present study is to evaluate, by a proteomic approach, the effects of oxidative stress, induced by UVB irradiation, on protein expression and specific protein oxidation in human keratinocytes transformed with the whole HPV-16 genome, namely HK-168 cells. UVB irradiation is unanimously recognized as the major source of oxidative stress and can generate the complete set of reactive oxygen species (ROS), including hydroxil radical, superoxide anion and hydrogen peroxide. Considering the lack of animal model of cervical cancers, the limited availability of tissue sampling and the unfeasibility of human lesions for progression studies, *in vitro* tissue cultures, and mostly HK-168, represent a convenient experimental model to study the early steps in HPV-driven carcinogenesis [17]. We focused our attention on oxidative damage occurring at protein level to identify proteins potentially involved in tumour progression. We analysed the protein expression profile and we identified the oxidatively modified proteins of UVB-treated cells compared with control cells. Our results provide new insight into the role of oxidative stress in cancer development.

Experimental procedures

Cell cultures

HK-168 cells were cultivated in keratinocyte serum-free medium in a humidified incubator at 37°C with 5% CO_2 (Invitrogen Life Technologies-San Giuliano Milanese, Italy) and passed 1: 3 twice a week. Before UVB treatment, cells were plated at a density of 80,000 cells/cm^2; after overnight incubation medium was removed and the monolayers were irradiated with a UVB dose of 20 J/m^2. Control cultures were decanted and sham irradiated. Five hours after irradiation, cells were pelleted and used for two-dimensional electrophoresis (2-DE) analysis.

Sample preparation

HK-168 cell pellets were lysated in 10 mM HEPES buffer (pH 7.4) containing 137 mM NaCl, 4.6 mM KCl, 1.1 mM KH_2PO_4, 0.1 mM EDTA and 0.6 mM $MgSO_4$ as well as proteinase inhibitors: leupeptin (0.5 mg/ml), pepstatin (0.7 μg/ml), type II S soybean trypsin inhibitor (0.5 μg/ml) and PMSF (40 μg/ml). Cell lysates were centrifuged at 14,000 × *g* for 10 min. to remove debris. Protein concentration in the supernatant was determined by the 'Coomassie Plus Protein Assay' (Pierce, Rockford, IL, USA).

Two-dimensional gel electrophoresis

Samples (150 μg) were incubated at room temperature for 30 min. either in four volumes of 10 mM 2,4-dinitrophenylhydrazine (DNPH) in 2 N HCl for protein carbonyl derivatization or 2 N HCl for gel maps and mass spectrometry analysis, according to the method of Levine *et al.* [18]. This was followed by precipitation of proteins by addition of ice-cold 100% trichloroacetic acid (TCA) to a final concentration of 15% and samples were placed on ice for 10 min. Precipitates were centrifuged at 15,800 × *g* for 2 min. The pellets were washed three times with 0.5 ml of 1: 1 (v/v) ethanol/ethyl acetate solution. After centrifugation and washing steps, the samples were dissolved with 200 μl of rehydration buffer (8 M urea, 20 mM dithiothreitol, 2.0% (w/v) CHAPS, 0.2% Biolytes, 2 M thiourea and bromophenol blue).

For the first-dimension electrophoresis, 200 μl of sample solution were applied to a ReadyStrip™ IPG strip pH 3–10 (Bio-Rad Laboratories, Milan, Italy). The strips were soaked in the sample solution for 1 hr to allow uptake of the proteins. The strips were then actively rehydrated in Protean IEF Cell Apparatus (Bio-Rad) for 16 hrs at 50V. The isoelectric focusing was performed at 300V for 2 hrs linearly; 500V for 2 hrs linearly; 1000 V for 2 hrs linearly, 8000 V for 8 hrs linearly and 8000 V for 10 hrs rapidly. All the processes above were carried out at room temperature. The focused IEF strips were stored at −80°C until second-dimension electrophoresis was performed.

For second-dimension electrophoresis, thawed strips were equilibrated for 10 min. in 50 mM Tris-HCl (pH 6.8) containing 6 M urea, 1% (w/v) sodium dodecyl sulphate (SDS), 30% (v/v) glycerol and 0.5% dithiothreitol, and then re-equilibrated for 15 min. in the same buffer containing 4.5% iodacetamide in place of dithiothreitol. Linear Gradient (8–16%) Precast criterion gels (Bio-Rad) were used to perform second-dimension electrophoresis. Precision Protein^{TM} Standards (Bio-Rad) were run along with the sample at 200 V for 65 min.

After electrophoresis, the gels were incubated in fixing solution (7% acetic acid, 10% methanol) for 20 min. Approximately 40 ml of Bio-Safe Coomassie Gel Stain (Bio-Rad) were used to stain the gels for 1 hr, on a gently continuous rocker. The gels were placed in deionized water overnight for destaining.

Western blotting

The same amount of protein samples (150 μg) was used for detecting specific protein carbonyl levels and the electrophoresis was carried out in the same way as described above. Proteins (150 μg) were incubated with 4 volumes of 20 mM 2,4-dinitrophenylhydrazine (DNPH) at room temperature for 20 min. The gels were prepared in the same manner as two-dimensional (2D)-electrophoresis. The proteins from the second-dimension electrophoresis gels were transferred to nitrocellulose (Bio-Rad) using Criterion Blotter apparatus (Bio-Rad) at 100 V for 1 hr. The 2,4-dinitrophenyl hydrazone (DNP) adducts of the carbonyls of the proteins were detected on the nitrocellulose paper using a primary rabbit antibody (Millipore Corp., MA, USA) specific for DNP-protein adduct (1: 100), followed by a secondary goat anti-rabbit IgG alkaline-phosphatase conjugated (Sigma, St. Louis, MO, USA) antibody. The resultant stain was developed using 5-bromo-4-chloro-3-indolyl phosphate/nitro blue tetrazolium (BCIP/NBT) solution (SigmaFast tablets; Sigma).

Image analysis

The 12 gels ($n = 6$ controls and $n = 6$ UVB-treated HK168 cells) and 12 nitrocellulose blots were scanned and saved in TIF format using a Scanjet 3300C (Hewlett Packard, Palo Alto, CA, USA). PDQuest 2D Analysis software (version 7.2.0, Bio-Rad) was used for matching and analysis of visualized protein spots among differential gels and membranes to compare protein and DNP immunoreactivity content between UV-treated HK-168 cells and control cells. To identify valid spots, PDQuest spot detection software was used with appropriate selection of the faintest and the smallest spots and a large representative section of the image containing spots, streaks and background gradations to make corrections for noise filter. Molecular mass and isoelectric point of the major spots were automatically determined by bilinear interpolation between landmark features on each image.

PDQuest software offers powerful comparative analysis and is specifically designed to analyse many gels or blots at once. Powerful automatching algorithms quickly and accurately match gels or blots and sophisticated statistical analysis tools identify experimentally significant spots. The principles of measuring intensity values by 2-D analysis software were similar to those of densitometric measurement. The average mode of background subtraction was used to normalize intensity values, which represents the amount of protein (total protein on gel and DNP-bound protein on the membrane) per spot.

Once spots were matched, images were manually edited to confirm proper spot detection and matching. The intensity of each protein spot was normalized as a percentage of total volume, corresponding to pixel intensity integrated over the area of each spot and divided by the sum of all spots in the gel to account for staining variability. Following manual editing and matching confirmation, average normalized spot volumes (pixel intensity over spot area) were compared between UVB-treated HK-168 cells and control cells. Target candidates were identified as protein spots that changed at least 1.5-fold between UVB-treated and control cells and that were either present or absent in one group or the other. Protein spots with greater than 50% internal variance were removed from the target list. Finally, remaining individual candidates were visually examined to ensure that the change was consistent in all gels.

After completion of spot matching, the normalized intensity of each protein spot from individual gels was compared between groups using statistical analysis. Statistical significance was assessed by a two-tailed Student's t-test, the method of statistical analysis most appropriate for proteomic analysis of small number of protein spots [19]. P-values < 0.05 were considered significant for comparison between control (control cells) and experimental data (UV-treated HK-168 cells).

Protein identification by mass spectrometry

Selected spots were manually excised from gels and submitted to trypsin proteolysis, as described by Mignogna *et al.* [20], with some difference. Briefly, after four destaining steps using 5% (30 min.), 50% (2 times, 30 min. each) and 100% (10 min.) acetonitrile in 25 mM ammonium bicarbonate, about 165 ng of trypsin (modified porcine variant, Promega, Madison, WI, USA), solubilized in 15 μl of a 25 mM ammonium bicarbonate digestion buffer, were added to each vacuum-dried gel spot. Digestion was performed at 37°C overnight. The peptide mixtures were eluted directly onto an appropriate MALDI target plate with 1.3 μl of α-cyano-4-hydroxy-*trans*-cinnamic acid matrix solution (2 mg/ml) in 70% acetonitrile containing 0.1% TFA (v/v). MALDI-ToF MS analyses were performed in a Voyager-DE STR instrument (Applied Biosystems, Framingham, MA, USA) equipped with a 337 nm nitrogen laser and operating in reflector mode. Mass data were obtained by accumulating several spectra from laser shots with an accelerating voltage of 20 kV. All mass spectra were externally calibrated using a standard peptide mixture containing des-Arg-bradykinin (*m/z* 904.4681), angiotensin I (*m/z* 1296.6853), 1–17 (*m/z* 2093.0867) and 18–39 (*m/z* 2465.1989) adrenocorticotropic hormone fragments. Two tryptic autolytic peptides were

also used for the internal calibration (*m/z* 842.5100 and 2807.3145). Several ion signals were submitted to fragmentation by post-source decay (PSD). PSD fragment ion spectra were obtained after isolation of selected precursor ions using timed ion selector (TIS), performing 10 steps of the reflectron voltage; for each individual step, the voltage was decreased of 25% of the previous step. The individual segments were automatically stitched together. The PSD fragment ions were measured as isotopically averaged masses. Calibration was performed with PSD spectra of angiotensin.

The MS and MS/MS data were analysed by MoverZ program (v. 2002, http: //bioinformatics.genomicsolutions.com), according to default parameters. Identification by peptide mass fingerprint (PMF), with the monoisotopic mass list obtained from each spot, after exclusion of expected contaminant mass values by Peak Erazor program (http: //www.protein.sdu.dk/gpmaw/Help/PeakErazor/peakerazor.html), was performed using the Mascot search engine (v. 2.1) against SwissProt database (v. 52.2, entries 263525). Up to one missed cleavage, 50 ppm measurement tolerance, oxidation at methionine (variable modification) and carbamidomethyl cysteine (fixed modification) were considered. Post-translational modifications were not considered. Identifications were validated when the probability-based Mowse protein score was significant according to Mascot [21]. If peptide matched to multiple members of a protein family, we reported the accession number of the protein identified as first hit (top rank) by Mascot. In case where all peptides detected were shared by individual proteins, as was the case of β-actin and γ-actin, this ambiguity was clearly indicated in the table.

Identification by tandem mass spectrometry analyses was performed using the Mascot search program (Version 2.1) against human SwissProt database (v. 54.6x, 290484 sequences; 107100015 residues; date 2008/01/03), with mass tolerance of ± 0.5 Da for the precursor ions and ± 0.8 Da for the fragment ions, with carbamidomethyl cysteine as fixed modification. The expectation value (E-value) for accepting identification by MS/MS spectra was set to <0.1, with a default significance threshold $P < 0.05$, that provides a level of 95% confidence.

A complete description of protein identification including MALDI-ToF spectra (Fig. S1), MS/MS spectra (Fig. S2) and mass peaks list (Table S1) is provided as Supporting Information.

Western blot analysis

The 40 ug of each protein sample was analysed with SDS-PAGE and electroblotted to PVDF membranes (Bio-Rad) using 25 mM Tris, 192 mM glycine and 20% (v/v) methanol. Protein transfer was carried out using a tank apparatus (Trans-blot cell, Bio-Rad) for a total of 2 hrs. Equal protein loading was confirmed by using 0.2% v/v Ponceau S in 7% acetic acid. The blotted membrane was blocked with 5% no-fat milk and reacted with a primary antibody (Anx2 from Abnova GmbH, Heidelberg, Germany; Hsp75 from Santa Cruz Biotech. Inc., Santa Cruz, CA, USA; ef1γ from Novus Biologicals Inc., Littleton, CO, USA; PDI A3 kindly provided by Prof. F. Altieri; Actin from Sigma). After washing with Tris-buffered saline containing 0.1% Tween 20, the membrane was incubated with horseradish peroxidase-conjugated secondary antibody at a dilution 1: 5000. Protein bands were visualized with ECL Plus™ (Amersham, NJ, USA) according to the manufacturer's protocol.

Immunoprecipitation

The immunoprecipitation was performed as described previously [22]. The antibodies were added directly to cell lysates with IP Buffer (NaCl 0.15M, NP-40 0.5%, Tris-HCl 50mM pH 7.2, protease inhibitors), and the mixture was incubated on a rotary mixer overnight at 4°C. The antigen/antibody complexes were precipitated with protein-A-conjugated agarose beads if the antibodies were raised in rabbit; protein G-conjugated agarose beads are used if the antibodies were raised in goat or mouse. Agarose beads were added in 50 μl aliquots from a stock of 300 mg/ml in PBS and mixed on a rotary mixer for 1 hr at room temperature. Beads were then centrifuged and washed with the washing buffer (pH 8, 50 mM Tris HCl, 150 mM NaCl, 0.1% Tween 20) three times. Proteins were solubilized in IEF rehydration buffer followed by 2D electrophoresis (annexin 2) or in sample buffer for post-Western blot analysis (Hsp75, Anx2 and ef1γ).

Post-Western blot immunochemical detection of protein carbonyl levels

The carbonyl levels of annexin2 (Anx2), heath shock protein 75 (Hsp75) and elongation factor 1 gamma (ef1γ) were detected by post-Western blot derivatization after immunoprecipitation [23]. Following the electroblotting procedure, the nitrocellulose membranes were equilibrated in 20% methanol for 5 min. Membranes were then incubated in 2 N HCl for 5 min. The membranes were next incubated in 0.5 mM DNPH solution exactly 5 min. The membranes were washed three times in 2 N HCl and five times in 50% methanol (5 min. each wash). After post-Western blot derivatization, the immunochemical detection and measurement of carbonyl levels of Anx2, Hsp75 and ef1γ were similar to that for total protein carbonyl level detection described above.

Statistical analysis

Two-sided, Student's t-tests were used to analyse differences in protein levels between UVB-treated HK-168 cell lysates and control cell lysates. A *P*-value of less than 0.05 was considered statistically significant. The significance of the change in carbonylation of specific proteins in the proteomics study was evaluated *via* nonparametric Mann–Whitney–Wilcoxon test. $P < 0.05$ was considered statistically significant. As discussed extensively by Maurer *et al.* [24], the proteome set of excessively carbonylated proteins with

only several protein spots is much smaller than microarray datasets with at least several thousand genes. Consequently, with this low number of proteins, microarray algorithms and statistical approaches are not applicable for proteomics, so we relied on the nonparametric Mann–Whitney–Wilcoxon for the small sample size.

Results

Protein profiling

2-DE offers an efficient tool for screening for abundant protein changes in different disease states as well as differences in metabolic pathways [25]. Protein profiling was conducted to identify proteins modulated by UVB using a 2-DE and Coomassie staining. In order to elucidate the effects of UVB treatment, we compared the differential patterns of protein expression between control untreated HK-168 cells and UVB-treated cells (Fig. 1A and B). The UVB dose (20 J/m^2) was chosen according to the results obtained in our previous studies [17], *i.e.* that dose able to induce an intermediate cell damage without suppressing the cell response mechanisms. The overall 2-D pattern of UVB-treated cells and control cells were similar (Fig. 1), however proteomics analysis revealed that some protein spots were down- or up-regulated by the UVB treatment. An enlarged image of one representative 2-D gel from control and UVB-treated HK-168 cells is also shown, with differentially expressed protein spots highlighted by circle and arrow (Fig. 2A and B). Statistically significant changes were defined as a minimum 1.5-fold increase or decrease in expression levels of a protein spot in UVB-treated HK-168 cells in comparison with control cells. To assess reproducibility, the correlation coefficients among six replicate gels were calculated. The average *r* value was 0.9, indicating high-quality 2DE gels as well as stable and reproducible culture and treatment conditions. Twenty proteins were found to be significantly modulated, among them 14 were up-regulated while 6 were down-regulated (Table 1).

The protein spots were excised from the gels, digested with trypsin, and then analysed by the MALDI-ToF. The resulting peptide mass fingerprints were used to identify the proteins by the Mascot search engine. The proteins identified to be up- and down-regulated are listed in Table 1. These spots were identified with good sequence coverage and significant protein scores.

Specific protein carbonyl level

The most widely studied oxidative stress-induced modification of proteins is the formation of carbonyl groups, which can occur by different mechanisms, including direct oxidation of side chains of lysine, arginine, proline and threonine residues, among others [26]. Western blot and subsequent immunochemical detection of

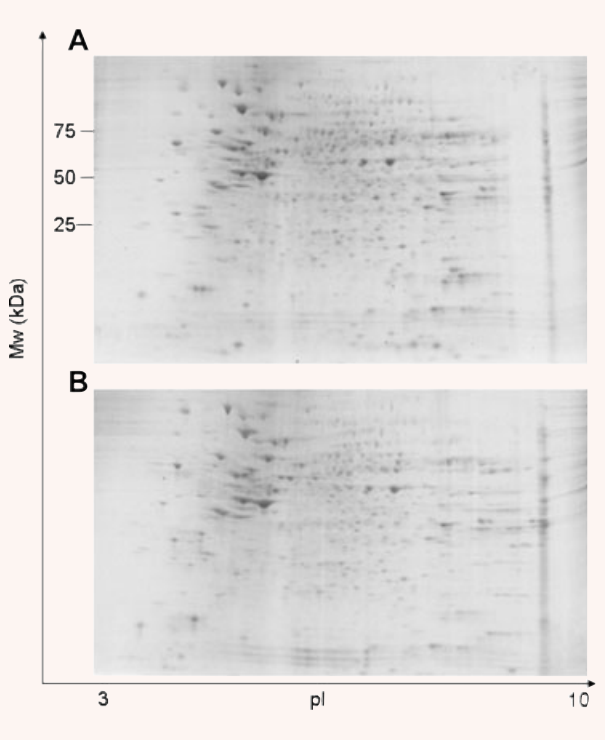

Fig. 1 Representative 2-D gels of control cells (**A**) and UVB-treated HK-168 cells (**B**). Proteins (150 μg) were separated on immobilized pH 3–10 IPG strips followed by separation on 8–16% gradient SDS-PAGE gels and stained with Biosafe Coomassie.

DNP-adducts allowed identification of carbonylated proteins in UVB-treated HK cells in comparison with untreated cells.

Oxidized proteins can be detected by WB because the protein-bound carbonyl groups react with DNPH and can be recognized by antibodies to the protein hydrazone. We used a parallel approach to quantify the protein levels by Bio-Safe Coomassie staining and the carbonyl levels by immunochemistry. The specific carbonyl levels were obtained by dividing the carbonyl level of a protein spot on the nitrocellulose membrane by the protein level of its corresponding protein spot on the gel. Such ratios give the carbonyl level per unit of protein.

Figure 3 shows representative 2D Western blots of control cells (a) and UVB-treated cells (b). In comparison with control cells, UV-treated HK-168 cells have five proteins significantly more oxidized. These proteins are: annexin 2 (Anx2), elongation factor Tu (efTu), elongation factor gamma (ef1γ), heat shock protein 75 (Hsp75) and α-enolase. Table 2 shows the proteins successfully identified by mass spectrometry along with the peptide matched number, percentage coverage, p*I*, Mw values and the increase of specific carbonyl levels, indexed as percentage of control. α-enolase was also identified in the same spot corresponding to ef1γ as shown

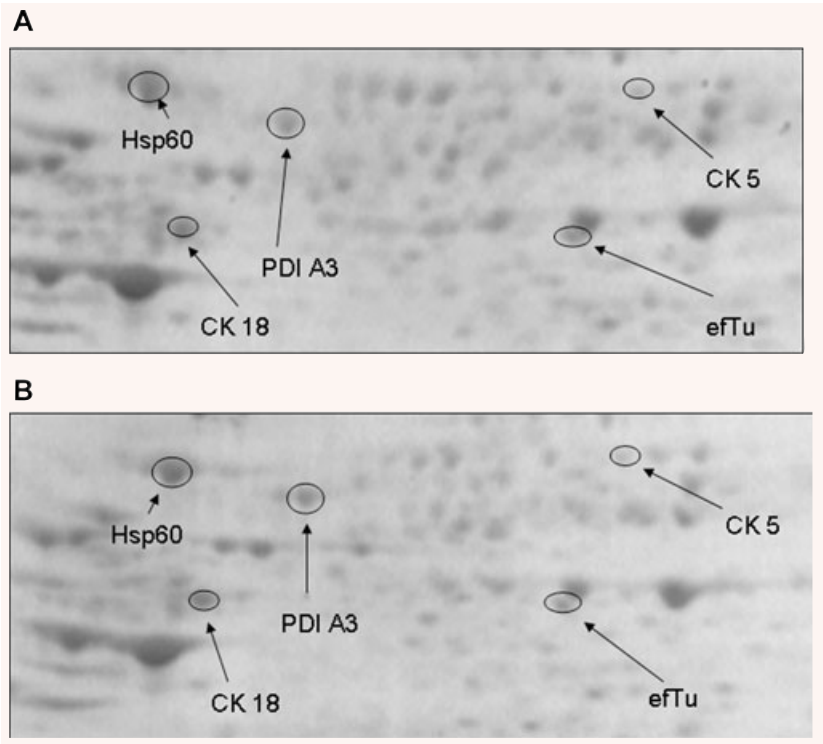

Fig. 2 Enlarged images of representative protein spots differentially expressed between UVB-treated HK-168 cells and control cells. Five representative spots are shown: PDI A3, CK 5 and CK 18, efTu and Hsp60. PDI A3 and efTu were down-regulated by UVB irradiation while CK5, CK 18 and Hsp60 were up-regulated in UVB-treated HK-168 cells.

by MALDI-ToF spectrum (Fig. S1). Specific oxidation of ef1γ was evaluated by post-Western immunodetection of carbonyl levels of immunoprecipitated protein.

Validation of identified proteins

To further verify the up- or down-regulation of the identified proteins, we performed Western blot analysis of some of the proteins we found modulated by UVB irradiation in HK-168 cells compared with control cells. Among these, we used specific antibodies against PDI A3, Anx2 and Hsp75. Figure 4 shows that all the above proteins showed the same pattern of expression of 2-DE (see Table 1). These results also strengthen the validation of 2-DE analysis in this report.

To validate the correct identification of protein spots, immunochemical selection of Anx2 was undertaken. Upon immunoprecipitation, the spot was absent in the 2D gels (Fig. 5). Thus, the identification of Anx2 was validated by immunochemistry, indicating that identification of proteins by mass spectrometry is equivalent to those by immunochemistry and providing confidence in the redox proteomics identification of the other carbonyl-modified proteins reported in this study.

Additionally, in order to confirm the protein identified by peptide mass fingerprints, PSD analysis of selected *m/z* values was performed. Fragmentation by PSD is a very powerful method for identifying proteins of which the sequence is available in databases. The analysis of PSD spectra allowed the unambiguously identification of efTu, oxygen-regulated protein precursor, Heterogeneous nuclear ribonucleoprotein F, Heterogeneous nuclear ribonucleoprotein C1/C2 and Hsp60. One representative PSD spectrum, in particular of the oxygen-regulated protein precursor, is shown in Fig. 6.

To validate the proteomics results, we used traditional immunochemistry to detect the oxidized proteins. Consistent with the proteomics results, the carbonyl levels of Hsp75, Anx2 and ef1γ were significantly increased by about 70%, 80% and 60%, respectively, in UVB-treated HK-168 cells compared to control cells (Fig. 7). The increased carbonyl levels of Anx2 and Hsp75 in UVB-treated HK-168 cells were more robust when detected by proteomics method. The differences in the magnitude of fold changes of carbonyl levels between the two techniques are likely because proteomics measures the carbonyl level per unit of protein, whereas Western blotting measures the carbonyl level of total protein. Clearly, both techniques showed that Anx2, Hsp75 and ef1γ are oxidatively modified in UVB-treated HK-168 cells, thus validating our proteomics results.

Discussion

Increasing evidence supports the role of oxidative stress in cancer development [1, 2]. Natural occurring HPV infection is unanimously recognized as the aetiological factor of cervical cancer

Table 1 Identification of UV-induced or -suppressed protein spots by mass spectrometry

Protein name	Fold change	AC(a)	Matched/ searched	MW (kDa)	pI	Coverage (%)	Protein score	Identification
Cytokeratin 19	↑	P08727	14/26	44	5.04	37	215	MS
Cytokeratin 8	↑	P05787	13/30	53	5.52	25	126	MS
Cytokeratin 18	↑	P05783	8/18	48	5.34	23	77	MS
Cytokeratin 5	↑	P13647	11/28	62	7.59	18	128	MS
Protein disulphide-isomerase A6	↓	Q15084	9/28	48.5	4.95	27	94	MS
Protein disulphide-isomerase A3	↓	P30101	18/28	57	5.98	41	175	MS
β-Actin or	↑	P60709	8/28	42	5.29	27	79	MS
γ- Actin		P63261			5.31			
Annexin 2	↓	P07355	16/53	39	7.57	52	127	MS
Enoyl CoA hydratase	↑	Q13011	8/15	36	8.16	32	140	MS
Succinyl-CoA:3-ketoacid-coenzyme A transferase 1*	↑	P55809	5/36	56	7.14	17	57	MS
ALDH, mitochondrial Precursor*	↑	P30807	8/39	57	6.36	22	59	MS
Hsp60	↑	P10809	12/34	61	5.7	34	107	MS-MS/MS
Hsp75	↑	Q12931	13/23	80	8.3	30	190	MS
Elongation factor Tu	↓	P49411	10/12	50	7.26	29	157	MS-MS/MS
Neutral alpha-glucosidase AB	↑	Q14697	27/46	107	5.74	34	251	MS
Oxygen regulated protein precursor	↑	Q9Y4L1	20/32	111.5	5.2	28	271	MS-MS/MS
Transitional endoplasmic reticulum ATPase	↑	P55072	8/13	90	5.14	11	80	MS
Heterogeneous nuclear ribonucleoprotein C1/C2	↓	P07910	6/12	33.7	4.95	15	87	MS-MS/MS
Heterogeneous nuclear ribonucleoprotein H3	↑	P31942	5/6	37	6.37	15	89	MS
Heterogeneous nuclear ribonucleoprotein F	↓	P52597	5/16	46	5.38	17	73	MS-MS/MS

The peptide mixtures obtained from the protein spots, treated with trypsin, were analysed by MALDI-ToF-MS and the relative mass lists used for identification by the Mascot program (Matrix Science). (a) AC = accession number (SwissProt). *Proteins identified in the same spot.
MS = identification by peptide mass fingerprint (PMF).
MS-MS/MS = identification by PMF and tandem mass spectrometry analysis (see text).

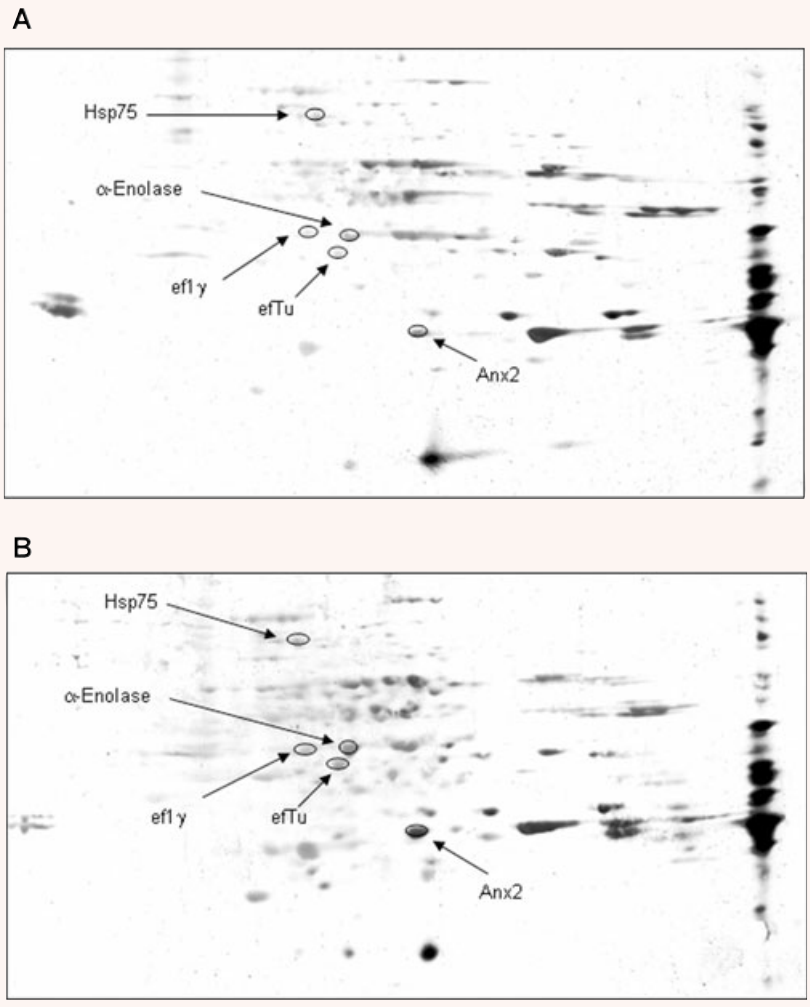

Fig. 3 Two-dimensional carbonyl immunoblots from UVB-treated HK-168 (**B**) cells and control cells (**A**). Positions of the five identified protein are shown on the blots. Relative change in carbonyl immunoreactivity, after normalization of the immunostaining intensities to the protein content, was significant for five proteins. See text.

Table 2 Summary of proteins identified as significantly oxidized in UVB-treated HK-168 cells compared with control cells

Oxidatively modified protein	AC(a)	Sequence coverage %	Matched/ searched	Protein Score	pI	MW (kDa)	Protein oxidation (%)*	*P*-value
efTu	P49411	29	10/12	157	7.26	49.85	350 ± 67	< 0.05
ef1γ	P26641	45	16/44	129	6.27	50.43	190 ± 40	< 0.05
Anx2	P07355	52	16/53	127	7.56	38.81	410 ± 65	< 0.05
Hsp75	Q12931	30	13/23	190	8.30	80.35	300 ± 40	< 0.05
α-Enolase	P06733	52	20/34	265	6.99	47.35	280 ± 54	< 0.02

*For each protein the carbonyl immunoreactivity/protein expression values were averaged ($n = 6$) and expressed as percent oxidation compared to control ± S.E.M. The *P*-value listed is the significance of elevated protein carbonyls relative to control samples (see text). (a) = accession number (SwissProt).

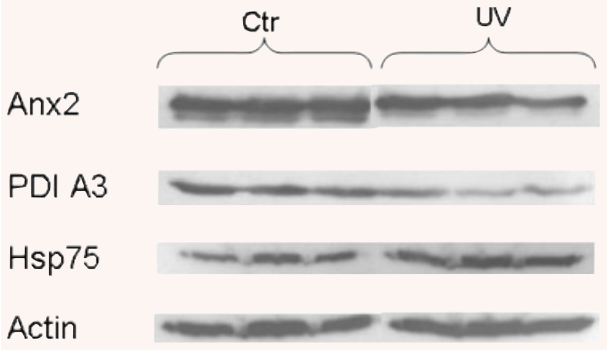

Fig. 4 Western blot for validation of identified proteins. Immunochemical selection of Anx2, Hsp75 and PDI A3 was undertaken. 40 μg of protein aliquots were loaded on 12% Tris gels and blotted with specific antibody against Anx2, Hsp75 and PDI A3. Western blot analysis confirmed proteomic results of increased levels of Hsp75 and decreased levels of Anx2 and PDI A3 in UVB-treated HK-168 cells compared with controls. Membranes were also probed for actin to show equal protein loading.

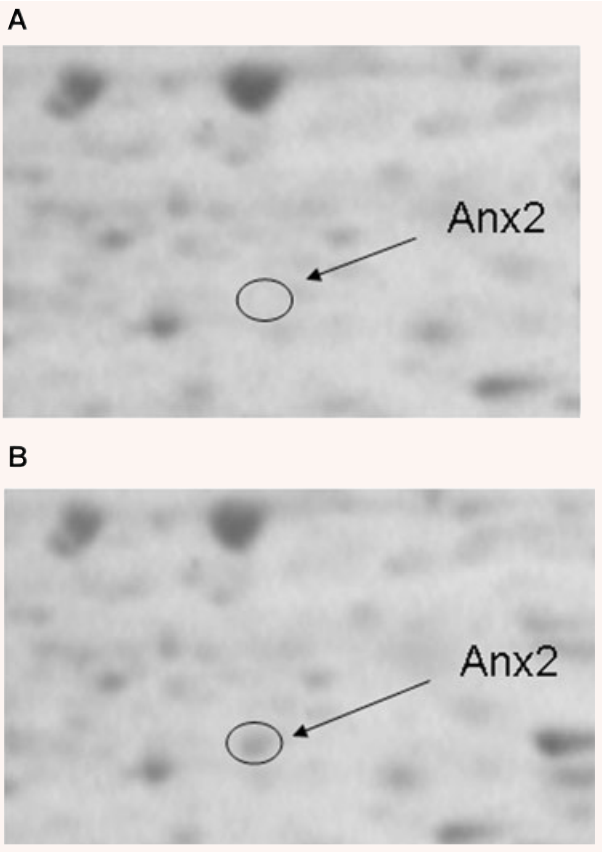

Fig. 5 (**A**) 2D electrophoresis gel from supernatant of HK-168 cells obtained after immunoprecipitation by anti-Anx2 antibody. (**B**) 2D electrophoresis gel from the same sample without immunoprecipitation. The *arrowhead* indicates that Anx2 disappears after immunoprecipitation, confirming its identity.

[27], the second prevalent cancer among women worldwide. Despite viral oncogenes are well known very powerful cancer initiating agents, the year-long latency occurring between HPV infection and the development of the full neoplastic phenotype indicates that additional factors have to co-operate with the viral oncogenes in the neoplastic progression. Thus, in addition to its importance in human health, cervical cancer represents an attractive field in experimental oncology allowing the study of environmental agents involved in the multistep malignant progression. HK-168 cells, a transformed non-tumoural continuous cell line [17], represent a convenient experimental model to study the molecular mechanisms of cancer progression in viral transformed pre-neoplastic cells. In the current study, we used a proteomic approach to identify proteins with differential expression as well as those specifically oxidatively modified upon UVB irradiation in HK-168 cells. Indeed, proteomics measures primarily high-abundance proteins, which are ideal tumour biomarkers because they can easily be measured and targeted.

We selected a UVB dose able to induce intermediate cell damage without suppressing the cell response mechanisms to surrogate the environmental sub-lethal stress that is assumed to promote the malignant progression in conjunction with the deregulated growth of HPV-infected cells. Consistently, we have recently demonstrated that under this subtoxic dose of UVB, HK-168 cells are able to suppress temporarily the viral oncogenes transcription resulting in an adaptive survival response [17].

Our results showed a modulation of the expression levels of Cytokeratins (CKs). We found that CK 5, 8, 18 and 19 were up-regulated upon UVB irradiation. The expression of certain keratin proteins in a cell at a given time is defined as its state of differentiation, and modulation of differentiation program has been well documented in cell transformation and cancer development [28]. Cytokeratins have been shown to be associated with invasive growth and progression to malignancy [29] in different types of human and murine epithelial tumours (including skin tumours), and even in tumours from nonepithelial origin. It has been well documented that cancer cells have altered keratin profiles – therefore altered differentiation programs – compared with their normal counterpart [28]; however, this phenomenon has not been fully understood. In our study, we speculate that increased expression of specific keratins represents an additional survival mechanism that counteract UVB-induced stress and may be responsible for the previously demonstrated apoptotic resistance of UVB-adapted HK-168 cells [17]. Because CK8 and CK19 are overexpressed in various cancer cells [30, 31], it is logical to assume that the elevation of these proteins could promote neoplastic cell survival as well as subsequent clonal expansion and then progression of tumour development.

The link of UVB-induced oxidative stress with cancer progression is further supported by our data on the expression levels of some chaperone proteins. Specifically, we found decreased levels of both proteins disulphide isomerase precursors A3 and A6 (PDI

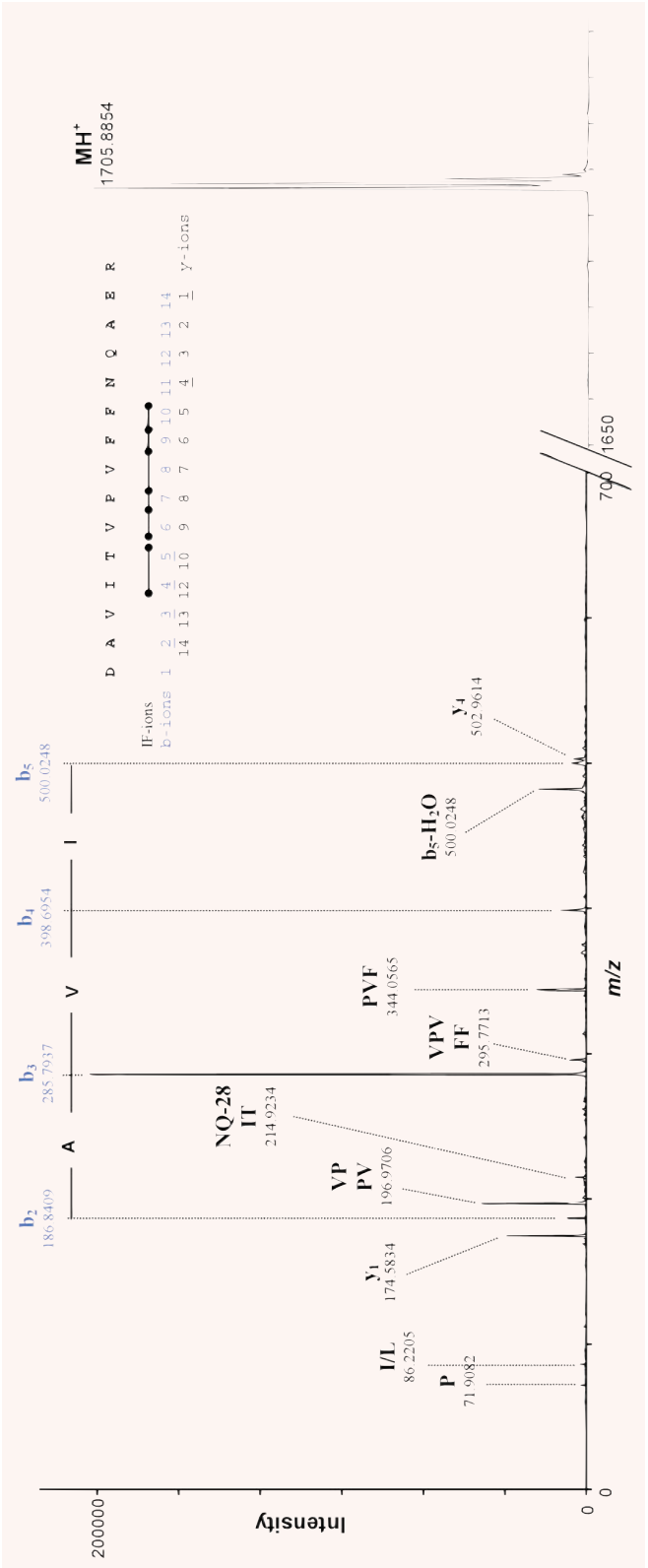

Fig. 6 A representative MALDI-ToF-PSD spectrum used to confirm protein identity: tandem mass analysis of 171–185 peptide (DAVITVPVFFNQAER, MH^+ at *m/z* 1705.8854) of the oxygen-regulated protein precursor. Peptide sequence coverage by *b* and *y* series ions and by internal fragment (IF) ions is indicated by underline.

A3 and PDI A6) and increased levels of Hsp60 and Hsp75 upon UVB irradiation. PDI is an enzyme that catalyses the formation and isomerization of disulphide bonds. It has peptide binding and chaperone activity for cell adhesion, and is involved in cell–cell interaction, gene expression, actin filament polymerization and regulation of reception functions. It was previously reported that the PDI expression is markedly increased in dying and apoptotic cells [32]. The finding of increased levels of Hps60 and Hsp75 is an agreement with current data indicating that Hsps are expressed in increased amounts in many cancers [33, 34] owing to the de-repression of their genes during malignant progression [35]. At these high levels, HSP family members play a facilitating role in cancer development by permitting autonomous growth, through the accumulation of overexpressed and mutated oncogenes and by inhibiting the programmed cell death of tumour cells [36]. Accordingly, Hsps expression is well associated with the resistance to cell death in various tumours [37]. Taken together, our results outline a consistent pattern of pro-carcinogenic modulation with repression of pro-apoptotic factors (PDI) and elevation of proliferative factors (Hsp).

Proteomics can also be utilized to analyse the post-translational modifications that regulate protein formation and function [38, 39]. By redox proteomics approach we identified five proteins that resulted oxidatively modified by UVB treatment in HK-168 cells: efTu, ef1γ, Anx2, Hsp75 and α-enolase. Numerous studies have demonstrated that protein oxidation impairs protein function [40–42]. In view of the fact that carbonylation is frequently associated with reduced or totally abrogated protein catalytic functions and triggering the formation of high molecular, potentially cytotoxic aggregates, this modification is likely to perturb cellular homeostatis [40]. Accumulation of modified proteins disrupts cellular function either by loss of catalytic and structural integrity or by perturbation of regulatory pathways. Although growing body of knowledge is currently available on the role of protein oxidation in the pathogenesis of neurodegenerative disorders [43, 44], so far little is known about the involvement of oxidative post-traslational modification of target proteins in cancer development. This is the first study to use a redox proteomics approach to investigate how protein oxidation may possibly contribute to cancer development.

efTu and elfγ are intimately involved in the protein synthesis machinery: efTu is a nuclear-encoded protein and functions in the translational apparatus of mitochondria [45]; ef1γ is an abundant protein required for the binding of aminoacyl-tRNAs to acceptor sites of ribosomes during protein synthesis [46] and its expression level is regulated in many situations such as growth arrest, transformation and aging [47]. Because of this regulation in various states of cell life and its key position in protein synthesis as well as cytoskeletal organization, ef1γ is an important determinant of cell proliferation and senescence. Our findings of increased carbonyl levels of efTu and ef1γ suggest an impairment of the protein synthesis machinery, either in the mithocondria or cytosol, associated with an impairment of the rate and specificity of ribosome functions. Numerous studies have provided indirect evidence that suggests alterations in protein synthesis may occur in pre-cancerous cells [48, 49]. In addition, it has been reported that oxidative damage may contribute to decreased protein synthesis [50]. We hypothesize that dysfunction of the protein synthesis apparatus, mediated in part by oxidative stress, could compromise the ability of cells to generate the various factors that are needed to regulate cell homeostasis thus contributing to the development of cancer.

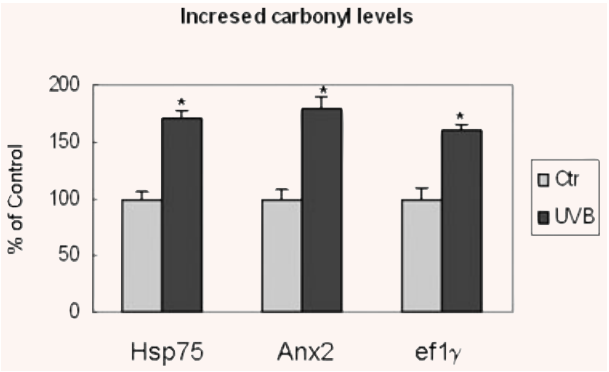

Fig. 7 Increased carbonyl level of Hsp75, Anx2 and ef1γ. Data represent the alteration of the Hsp75, Anx2 and ef1γ carbonyl levels in UV-treated HK-168 cells compared to control cells using traditional immunochemical detection. Error bars indicate S.E.M for 3 samples in each group. Measured values are normalized with the mean of the control cells. $^*P < 0.05$.

We also found that Anx2 showed a significant increase of carbonyl levels in UVB-irradiated HK-168 cells compared with control cells. Annexins are a family of Ca^{2+}- and membrane-binding proteins to which several biological functions have been assigned [51, 52] and recent studies suggest that Anx2 might be linked to tumourigenesis [53]. Based on the existence of redox-sensitive cysteine [54], Anx2 is an oxidatively labile protein whose level of activity is regulated by the redox status of its sulphydryl groups. We hypothesize that the increased carbonyl levels might alter the redox status of the protein thus leading to dysfunction of its biological activity. We also found decreased levels of Anx2 in UVB treated HK-168 cells. Since overexpression of the Anx2 gene is commonly observed in both virally transformed cell lines and human tumours [55], our finding might appear contradictory. We suggest that the down-regulation of protein level could be explained as a compensatory mechanism towards increased protein oxidation. Indeed, the activity of Anx2 is crucially regulated by its redox status and secondly by its expression levels. However, further studies are needed to elucidate the role that down-regulation and oxidation of Anx2 could have on cellular transformation induced by UVB-irradiation.

The oxidation of particular chaperones is an important event during oxidative stress and several studies demonstrated the specific oxidation of different chaperones depending on the particular stress condition [56], in the effort to reduce the toxic effects of oxidative stress. Considering that protein oxidation reasonably results in alteration of protein function [57], the increased carbonyl levels of Hsp75 found in HK-168 cells upon UVB irradiation may favour the accumulation of misfolded proteins. The increased

oxidation of Hsp75, together with its increased expression, may contribute to select a malignant cell phenotype characterized by increasing amount of misfolded, hence dis-regulated, proteins with increased resistance to apoptotic death.

The oxidation of α-enolase, the only glicolytic enzyme to be carbonylated in our study, is well documented by several reports showing its susceptibility to different conditions of oxidative stress [58–60]. We suggest that the selective damage of α-enolase could be related to its structure and therefore could not be considered a specific event in the carcinogenesis process.

The aim of our proteomic study was to elucidate the role of oxidative stress as a concurrent agent in the malignant transformation of HPV-transformed cells. We have identified selective protein targets that are modulated, either at protein level or post-traslationally modified, upon a stress stimulus such as UV irradiation.

In conclusion, our results indicate that oxidative stress induced by UVB irradiation evokes an orchestrated response affecting multiple cellular pathways that might contribute to the carcinogenesis mechanisms in HPV-infected cells.

Acknowledgements

This study was supported in part by a grant from the Ministry of Health of Italy and by FIRB [RBIN04T7MT_001] to M.E.S. The authors wish to thank Dr. Aldo Venuti for having kindly supplied the HK-168 cells, Dr. Daniela Di Sciullo and Mr. Vincenzo Peresempio for skilled technical assistance.

Supporting Information

Additional Supporting Information may be found in the online version of this article:

Fig. S1 MALDI-TOF mass spectra of identified proteins: The masses belonging to identified proteins are reported, as well as the position of the corresponding peptides in the sequence. Presence of oxidized Methionine (Mox) is also indicated. When the PMF of a single spot yielded a double identification, the mass values of each component are indicated with ([a]) and ([b]) letters, respectively.

Fig. S2 MS/MS spectra of (A) Heterogeneous nuclear ribonucleoprotein F; (B) Hsp60, mitochondrial precursor; (C) Heterogeneous nuclear ribonucleoproteins C1/C2; (D) Elongation factor Tu, mitochondrial precursor. IF-ions (internal fragment ions), b and y-ions revealed in MS/MS spectra are underlined in sequence. In each spectrum the Mascot result is also reported.

Table S1 Protein identified by peptide mass fingerprint (PMF), using the Mascot search engine. The monoisotopic mass list, automatically obtained from MoverZ spectra, for each protein is reported. The mass lists contain *m/z* values belonging to the identified proteins (bold), and *m/z* not matched. When the PMF of a single spot yielded a double identification, the mass values of each component are indicated with ([a]) and ([b]) letters. *Both proteins were found to be carbonylated (see text)

This material is available as part of the online article from: http://www.blackwell-synergy.com/doi/abs/10.1111/j.1582-4934.2008.00465.x
(This link will take you to the article abstract).

Please note: Wiley-Blackwell are not responsible for the content or functionality of any supporting materials supplied by the authors. Any queries (other than missing material) should be directed to the corresponding author for the article.

References

1. **Valko M, Rhodes CJ, Moncol J, *et al.*** Free radicals, metals and antioxidants in oxidative stress-induced cancer. *Chem Biol Interact.* 2006; 160: 1–40.
2. **Karihtala P, Soini Y.** Reactive oxygen species and antioxidant mechanisms in human tissues and their relation to malignancies. *Apmis.* 2007; 115: 81–103.
3. **Halliwell B.** Oxidative stress and cancer: have we moved forward? *Biochem J.* 2007; 401: 1–11.
4. **D'Autreaux B, Toledano MB.** ROS as signalling molecules: mechanisms that generate specificity in ROS homeostasis. *Nat Rev Mol Cell Biol.* 2007; 8: 813–24.
5. **Kamata H, Hirata H.** Redox regulation of cellular signalling. *Cell Signal.* 1999; 11: 1–14.
6. **Ryter SW, Kim HP, Hoetzel A, *et al.*** Mechanisms of cell death in oxidative stress. *Antioxid Redox Signal.* 2007; 9: 49–89.
7. **Toyokuni S, Okamoto K, Yodoi J, *et al.*** Persistent oxidative stress in cancer. *FEBS Lett.* 1995; 358: 1–3.
8. **Storz P.** Reactive oxygen species in tumor progression. *Front Biosci.* 2005; 10: 1881–96.
9. **Szatrowski TP, Nathan CF.** Production of large amounts of hydrogen peroxide by human tumor cells. *Cancer Res.* 1991; 51: 794–8.
10. **Saeki K, Kobayashi N, Inazawa Y, *et al.*** Oxidation-triggered c-Jun N-terminal kinase (JNK) and p38 mitogen-activated protein (MAP) kinase pathways for apoptosis in human leukaemic cells stimulated by epigallocatechin-3-gallate (EGCG): a distinct pathway from those of chemically induced and receptor-mediated apoptosis. *Biochem J.* 2002; 368: 705–20.
11. **Kim SW, Han YW, Lee ST, *et al.*** A superoxide anion generator, pyrogallol, inhibits the growth of HeLa cells *via* cell cycle arrest and apoptosis. *Mol Carcinog.* 2008; 47: 114–125.
12. **Ozben T.** Oxidative stress and apoptosis: impact on cancer therapy. *J Pharm Sci.* 2007; 96: 2181–96.
13. **Hensley K, Robinson KA, Gabbita SP, *et al.*** Reactive oxygen species, cell signaling, and cell injury. *Free Radic Biol Med.* 2000; 28: 1456–62.
14. **zur Hausen H.** Papillomaviruses and cancer: from basic studies to clinical application. *Nat Rev Cancer.* 2002; 2: 342–50.

15. **Fehrmann F, Laimins LA.** Human papillomaviruses: targeting differentiating epithelial cells for malignant transformation. *Oncogene.* 2003; 22: 5201–7.
16. **zur Hausen H.** Papillomaviruses causing cancer: evasion from host-cell control in early events in carcinogenesis. *J Natl Cancer Inst.* 2000; 92: 690–8.
17. **De Marco F, Perluigi M, Foppoli C, *et al.*** UVB irradiation down-regulates HPV-16 RNA expression: implications for malignant progression of transformed cells. *Virus Res.* 2007; 130: 249–59.
18. **Levine RL, Williams JA, Stadtman ER, *et al.*** Carbonyl assays for determination of oxidatively modified proteins. *Methods Enzymol.* 1994; 233: 346–57.
19. **Maurer HH, Peters FT.** Toward high-throughput drug screening using mass spectrometry. *Ther Drug Monit.* 2005; 27: 686–8.
20. **Mignogna G, Giorgi A, Stefanelli P, *et al.*** Inventory of the proteins in Neisseria meningitidis serogroup B strain MC58. *J Proteome Res.* 2005; 4: 1361–70.
21. **Pappin DJ.** Peptide mass fingerprinting using MALDI-TOF mass spectrometry. *Methods Mol Biol.* 2003; 211: 211–9.
22. **Lauderback CM, Hackett JM, Huang FF, *et al.*** The glial glutamate transporter, GLT-1, is oxidatively modified by 4-hydroxy-2-nonenal in the Alzheimer's disease brain: the role of Abeta1–42. *J Neurochem.* 2001; 78: 413–6.
23. **Conrad CC, Talent JM, Malakowsky CA, *et al.*** Post-electrophoretic identification of oxidized proteins. *Biol Proced Online.* 2000; 2: 39–45.
24. **Maurer MH, Feldmann RE Jr, Bromme JO, *et al.*** Comparison of statistical approaches for the analysis of proteome expression data of differentiating neural stem cells. *J Proteome Res.* 2005; 4: 96–100.
25. **Butterfield DA, Castegna A.** Proteomics for the identification of specifically oxidized proteins in brain: technology and application to the study of neurodegenerative disorders. *Amino Acids.* 2003; 25: 419–25.
26. **Stadtman ER, Berlett BS.** Reactive oxygen-mediated protein oxidation in aging and disease. *Chem Res Toxicol.* 1997; 10: 485–94.
27. **Bosch FX, Manos MM, Munoz N, *et al.*** Prevalence of human papillomavirus in cervical cancer: a worldwide perspective. International biological study on cervical cancer (IBSCC) Study Group. *J Natl Cancer Inst.* 1995; 87: 796–802.
28. **Prasad S, Soldatenkov VA, Srinivasarao G, *et al.*** Intermediate filament proteins during carcinogenesis and apoptosis (Review). *Int J Oncol.* 1999; 14: 563–70.
29. **Barak V, Goike H, Panaretakis KW, *et al.*** Clinical utility of cytokeratins as tumor markers. *Clin Biochem.* 2004; 37: 529–40.
30. **Nagai T, Murota M, Nishioka M, *et al.*** Elevation of cytokeratin 19 fragment in serum in patients with hepatoma: its clinical significance. *Eur J Gastroenterol Hepatol.* 2001; 13: 157–61.
31. **Gharib TG, Chen G, Wang H, *et al.*** Proteomic analysis of cytokeratin isoforms uncovers association with survival in lung adenocarcinoma. *Neoplasia.* 2002; 4: 440–8.
32. **Prasad SC, Soldatenkov VA, Kuettel MR, *et al.*** Protein changes associated with ionizing radiation-induced apoptosis in human prostate epithelial tumor cells. *Electrophoresis.* 1999; 20: 1065–74.
33. **Calderwood SK, Khaleque MA, Sawyer DB, *et al.*** Heat shock proteins in cancer: chaperones of tumorigenesis. *Trends Biochem Sci.* 2006; 31: 164–72.
34. **Kimura E, Enns RE, Thiebaut F, *et al.*** Regulation of HSP60 mRNA expression in a human ovarian carcinoma cell line. *Cancer Chemother Pharmacol.* 1993; 32: 279–85.
35. **Jolly C, Morimoto RI.** Role of the heat shock response and molecular chaperones in oncogenesis and cell death. *J Natl Cancer Inst.* 2000; 92: 1564–72.
36. **Aghdassi A, Phillips P, Dudeja V, *et al.*** Heat shock protein 70 increases tumorigenicity and inhibits apoptosis in pancreatic adenocarcinoma. *Cancer Res.* 2007; 67: 616–25.
37. **Ciocca DR, Calderwood SK.** Heat shock proteins in cancer: diagnostic, prognostic, predictive, and treatment implications. *Cell Stress Chaperones.* 2005; 10: 86–103.
38. **Mann M, Jensen ON.** Proteomic analysis of post-translational modifications. *Nat Biotechnol.* 2003; 21: 255–61.
39. **Spickett CM, Pitt AR, Morrice N, *et al.*** Proteomic analysis of phosphorylation, oxidation and nitrosylation in signal transduction. *Biochim Biophys Acta.* 2006; 1764: 1823–41.
40. **Dean RT, Fu S, Stocker R, *et al.*** Biochemistry and pathology of radical-mediated protein oxidation. *Biochem J.* 1997; 324: 1–18.
41. **Stadtman ER.** Protein oxidation and aging. *Science.* 1992; 257: 1220–4.
42. **Smith CD, Carney JM, Starke-Reed PE, *et al.*** Excess brain protein oxidation and enzyme dysfunction in normal aging and in Alzheimer disease. *Proc Natl Acad Sci USA.* 1991; 88: 10540–3.
43. **Butterfield DA, Kanski J.** Brain protein oxidation in age-related neurodegenerative disorders that are associated with aggregated proteins. *Mech Ageing Dev.* 2001; 122: 945–62.
44. **Perluigi M, Poon HF, Maragos W, *et al.*** Proteomic analysis of protein expression and oxidative modification in r6/2 transgenic mice: a model of Huntington disease. *Mol Cell Proteomics.* 2005; 4: 1849–61.
45. **Ling M, Merante F, Chen HS, *et al.*** The human mitochondrial elongation factor tu (EF-Tu) gene: cDNA sequence, genomic localization, genomic structure, and identification of a pseudogene. *Gene.* 1997; 197: 325–36.
46. **Janssen GM, Morales J, Schipper A, *et al.*** A major substrate of maturation promoting factor identified as elongation factor 1 beta gamma delta in Xenopus laevis. *J Biol Chem.* 1991; 266: 14885–8.
47. **Mimori K, Mori M, Tanaka S, *et al.*** The overexpression of elongation factor 1 gamma mRNA in gastric carcinoma. *Cancer.* 1995; 75: 1446–9.
48. **Lee JM.** The role of protein elongation factor eEF1A2 in ovarian cancer. *Reprod Biol Endocrinol.* 2003; 1: 69.
49. **Tomlinson VA, Newbery HJ, Wray NR, *et al.*** Translation elongation factor eEF1A2 is a potential oncoprotein that is overexpressed in two-thirds of breast tumours. *BMC Cancer.* 2005; 5: 113.
50. **Ding Q, Markesbery WR, Chen Q, *et al.*** Ribosome dysfunction is an early event in Alzheimer's disease. *J Neurosci.* 2005; 25: 9171–5.
51. **Waisman DM.** Annexin II tetramer: structure and function. *Mol Cell Biochem.* 1995; 149–150: 301–22.
52. **Moss SE.** Annexins. *Trends Cell Biol.* 1997; 7: 87–9.
53. **Mai J, Waisman DM, Sloane BF.** Cell surface complex of cathepsin B/annexin II tetramer in malignant progression. *Biochim Biophys Acta.* 2000; 1477: 215–30.
54. **Tanaka T, Akatsuka S, Ozeki M, *et al.*** Redox regulation of annexin 2 and its implications for oxidative stress-induced renal carcinogenesis and metastasis. *Oncogene.* 2004; 23: 3980–9.
55. **Ozaki T, Sakiyama S.** Molecular cloning of rat calpactin I heavy-chain cDNA whose expression is induced in v-src-transformed rat culture cell lines. *Oncogene.* 1993; 8: 1707–10.

56. **Choi J, Conrad CC, Dai R, *et al.*** Vitamin E prevents oxidation of antiapoptotic proteins in neuronal cells. *Proteomics.* 2003; 3: 73–7.
57. **Butterfield DA, Perluigi M, Sultana R.** Oxidative stress in Alzheimer's disease brain: new insights from redox proteomics. *Eur J Pharmacol.* 2006; 545: 39–50.
58. **Cabiscol E, Piulats E, Echave P, *et al.*** Oxidative stress promotes specific protein damage in Saccharomyces cerevisiae. *J Biol Chem.* 2000; 275: 27393–8.
59. **Castegna A, Aksenov M, Thongboonkerd V, *et al.*** Proteomic identification of oxidatively modified proteins in Alzheimer's disease brain. Part II: dihydropyrimidinase-related protein 2, alpha-enolase and heat shock cognate 71. *J Neurochem.* 2002; 82: 1524–32.
60. **Tamarit J, Cabiscol E, Ros J.** Identification of the major oxidatively damaged proteins in *Escherichia coli* cells exposed to oxidative stress. *J Biol Chem.* 1998; 273: 3027–32.